Material Science Research India Vol. **4**(2), 413-420 (2007)

Electrical transport study of superionic system Li_3PO_4 : *X* Li_3VO_4

RAJESH KUMAR PATEL, SATYENDRA SINGH and KANCHAN GAUR

Department of Physics, K.N. Government P.G. College, Gyanpur, Bhadohi (India).

(Received: October 16, 2007; Accepted: December 15, 2007)

ABSTRACT

Measurement of electrical conductivity (σ) and Seebeck coefficient (S) have been performed on the solidified melt of the lithium based superionic system Li_3PO_4 : *x* Li_3VO_4 where x = 0.0, 0.33, 0.50, 0.67, 1.0, 1.5 and 2.0 in the temperature range 500 K to the melting point of the materials. All the studied materials are purely ionic in superionic phase which has been observed below their melting point. At phase transition solids undergo from normal to superionic phase. Ionic and electronic parts of electrical conductivity have also been separated. These solids are mixed conductors in normal phase. Electrical conduction mechanism have also been discussed..

Keywords : Electrical transport, superionic system, electrical conductivity, seebeck coefficient.

INTRODUCTION

Extensive studies have been done by many workers[1-7] in the search of lithium ion conducting superionic solids because of their potentialities in high power miniaturized solid state batteries[8-15]. We have already made attempts in this direction[16-20]. This paper reports transport studies of solidified melt of the system Li_3PO_4 : *x* Li_3VO_4 with x = 0, 0.33, 0.50, 0.67, 1.0, 1.5 and 2.0 in the wide temperature range.

Material preparation and experimental technique

The starting materials for the studied system were Li_3PO_4 and Li_3VO_4. The base materials Li_2O, P_2O_5 and V_2O_5 for the preparation of Li_3VO_4 and Li_3PO_4 were procured from Rare and Research Chemicals, Bombay and Chempure, Calcutta with stated purity of 99.999%. Base materials were taken in stiochiometric amount and were fired at 1100 K in air in a silica crucible for 48 h with one intermediate grinding. Then they were melted and cooled slowly to room temperature. The firing temperature was same for both the materials Li_3VO_4 and Li_3PO_4. X-ray diffraction pattern of these materials show that no uncreated starting material was left and single phase compound is prepared.

The compounds of the system Li_3PO_4 : *x* Li_3PO_4 were prepared by mixing the required amount of Li_3VO_4 and Li_3PO_4. The mixture was melted shaken thoroughly and cooled slowly to solidify. The measurement of electrical conductivity (σ) and Seebeck coefficient (S) was done on solidified melt. The details of electrodes used, sample holder and measuring techniques have been described else where[8, 20].

RESULT AND DISCUSSION

The electrical conductivity (s) and Seebeck coefficient (S) has been measured on at least two samples of different lots corresponding to particular value of x. No significant difference has been found between the values of both s and S of the

compounds from different lots. This shows that mixed compounds are not very sensitive to the method of preparation. The results of s and S variation with temperature are shown in Figs. 1-4 as Log σT and S vs T^{-1} plots. It is seen from these figures that plots are linear at lower temperature but shows faster increase above a certain temperature and then again shows a linear region. The linear temperature regions can be represented by eqs.

$$T\sigma = C\exp.\left(\frac{-E_a}{kT}\right) \qquad ...(1)$$

and

...(2)

where C is pre-exponential constant, E_a is activation energy, η is the slope of S vsT^{-1} plot, H is the intercept and other symbols have their usual meanings. The values of C, E_a and break temperature T_1 and T_2 are given in Table 1 whereas values of T_1^1, T_2^1 together with η and H are given in Table 2.

It is seen from Table 1 and 2 that break temperatures T_1 and T_2 observed from σ plots have no resemblance with break temperatures T_1^1, and T_2^1 observed from S vs T^{-1} plots. This may not be surprising as we expect these solids to be mixed conductors. All charge carriers irrespective of their nature will enhance σ but they will not do so for S. To know the nature of conductivity (ionic + electronic) we have performed the measurement of σ_{dc} at constant field and temperature as a function of time. The results have been plotted as log σ vs time plot Fig. 5 and 6. All the plots are of similar nature. The general trend is that σ_{dc} decreases with time and tends to become constant. This constancy is achieved after a short time at lower temperature compared to higher temperature. The value of σ_{dc} at

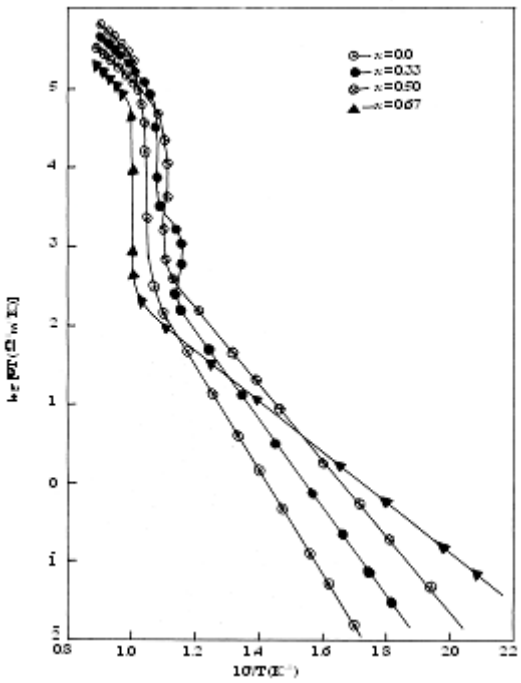

Fig. 1: Plots of logarithm of product of electrical conductivity and absolute temperature (log σT) against inverse of absolute temperature (T^{-1}) of the system Li_3PO_4 : *x* Li_3 VO_4

S

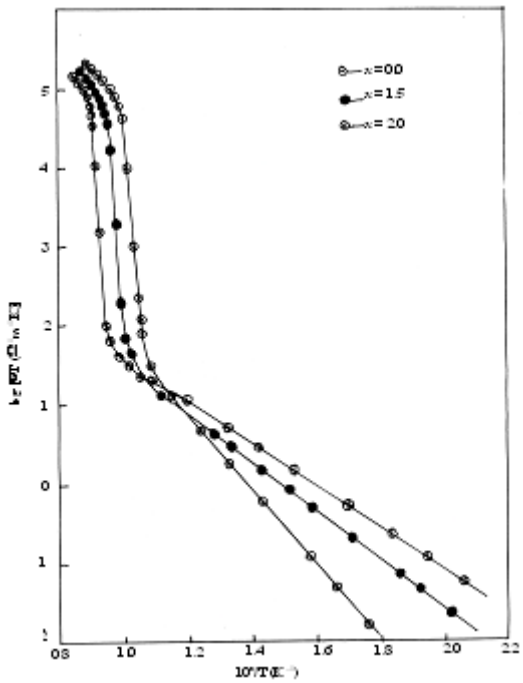

Fig. 2: Plots of logarithm of product of electrical conductivity and absolute temperature (log σT) against inverse of absolute temperature (T^{-1}) of the system Li_3PO_4 : *x* Li_3 VO_4

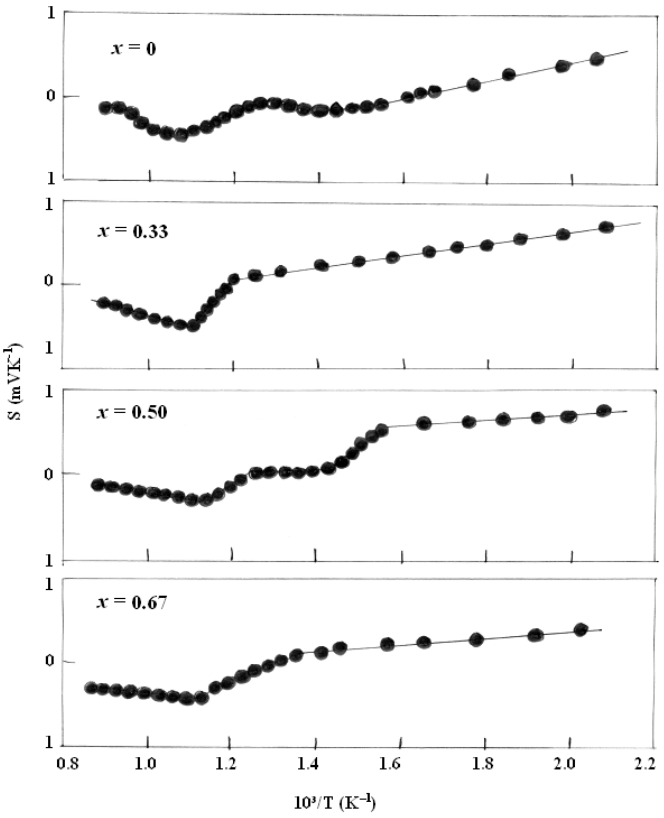

Fig. 3: Plots of Seebeck coefficient (S) against inverse of absolute temperature (T^{-1}) of the system Li_3PO_4 : *x* Li_3 VO_4

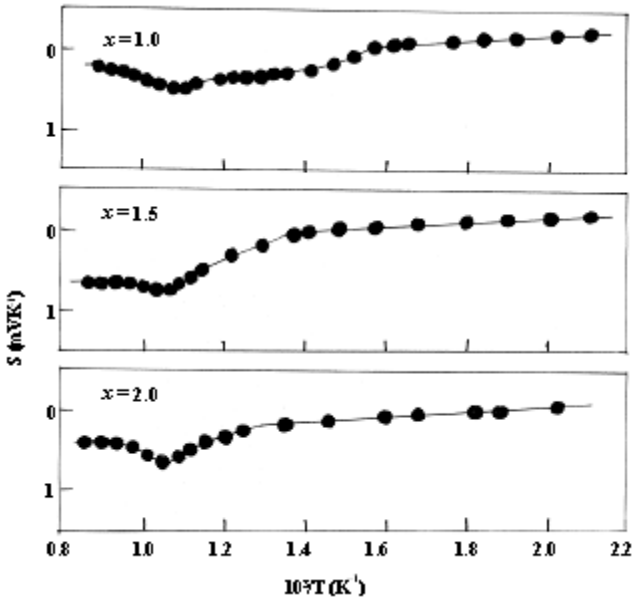

Fig. 4: Plots of Seebeck coefficient (S) against inverse of absolute temperature (T^{-1}) of the system Li_3PO_4 : *x* Li_3 VO_4

Table 1: Summarized results of electrical conductivity of studied system Li_3PO_4 : *x* Li_3VO_4

Material with x	Lower temperature range			Higher temperature range		
	E_a (eV)	C ($\Omega^{-1}m^{-1}K$)	T_1 (K)	T_2 (K)	E_a (eV)	C ($\Omega^{-1}m^{-1}K$)
0.0	1.32	2.90×10^7	865	1015	0.58	1.50×10^8
0.33	1.30	4.07×10^7	870	1020	0.56	8.12×10^7
0.50	1.28	3.65×10^7	885	1020	0.50	6.70×10^7
0.67	1.27	3.24×10^7	910	1025	0.54	5.15×10^7
1.0	1.25	2.21×10^7	917	1025	0.48	3.21×10^7
1.5	1.18	4.85×10^7	935	1030	0.50	6.08×10^6
2.0	1.07	5.19×10^7	945	1035	0.52	4.25×10^6

Table 2: Summarized results of Seebeck coefficient of studied system Li_3PO_4 : *x* Li_3VO_4

Material with x	Lower temperature range			Higher temperature range		
	η (eV)	H (mvK^{-1})	$T_1^{'}$ (K)	$T_2^{'}$ (K)	η (eV)	H (mvK^{-1})
0.0	0.44	– 0.56	640	960	– 1.64	1.32
0.33	0.46	– 0.70	660	935	– 1.52	1.25
0.50	0.42	– 0.75	645	910	– 0.80	1.30
0.67	0.38	– 0.40	690	900	– 0.72	1.20
1.0	0.35	– 0.32	640	950	– 1.08	1.18
1.5	0.31	– 0.22	700	945	– 0.68	0.90
2.0	0.25	– 0.10	740	940	– 0.62	1.10

Table 3: Span of superionic phase, melting point and phase transition temperature of studied system Li_3PO_4 : *x* Li_3VO_4

Material with x	Temperature span T (K)	T_m(K)	T_p (K)
0.0	1015 – 1110	1110	955 ± 5
0.33	1020 – 1130	1130	960 ± 5
0.50	1020 – 1145	1145	965 ± 5
0.67	1025 – 1165	1165	970 ± 5
1.0	1025 – 1180	1180	985 ± 5
1.5	1030 – 1190	1190	995 ± 5
2.0	1035 – 1195	1195	1010 ± 5

Table 4: Summarized results of electronic contribution to σ of the studied system Li_3PO_4 : *x* Li_3VO_4

Materialswith *x*	W (eV)	σ_0 ($\Omega^{-1}m^{-1}k$)	Linear temp. region T (K)
0.0	0.73	6.30×10^4	580 – 850
0.33	0.86	8.70×10^4	550 – 865
0.50	0.92	1.20×10^5	510 – 875
0.67	1.05	4.60×10^4	470 – 900
1.0	1.10	5.90×10^4	560 – 905
1.5	0.98	3.85×10^4	480 – 920
2.0	0.85	1.72×10^4	470 – 930

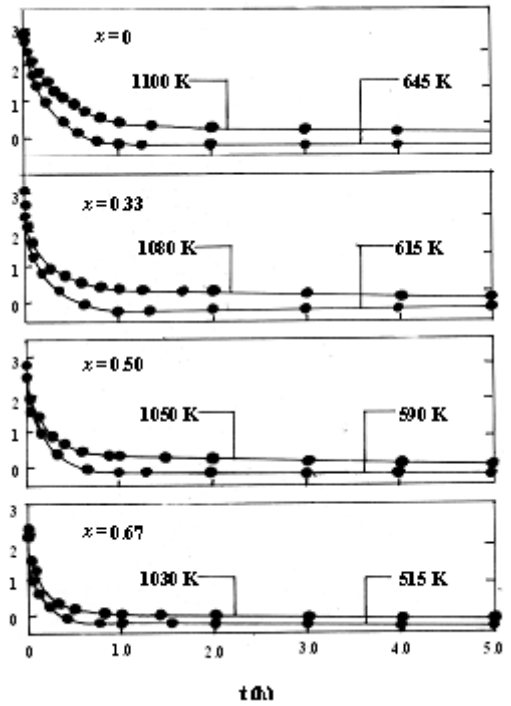

Fig. 5: Plots of logarithm of electrical conductivity (log σ) against time (t) of the system Li_3PO_4 : *x* Li_3 VO_4

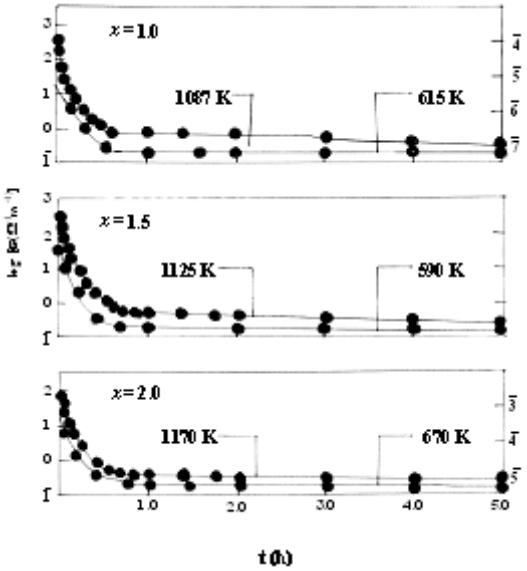

Fig. 6: Plots of logarithm of electrical conductivity (log σ) against time (t) of the system Li_3PO_4 : *x* Li_3 VO_4

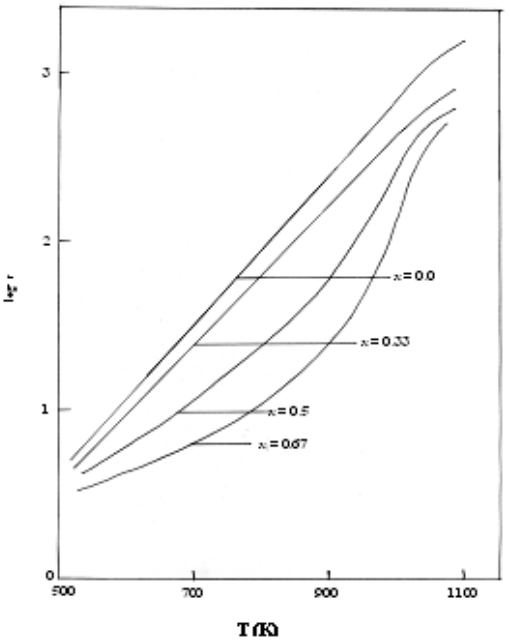

Fig. 7: Plots of logarithm of ratio of ionic to electronic conductivity (log r) against absolute temperature (T) of the system Li_3PO_4 : *x* Li_3 VO_4

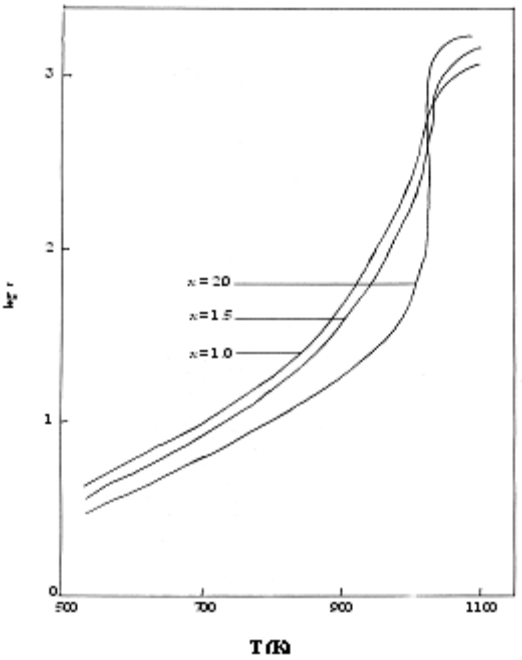

Fig.. 8: Plots of logarithm of ratio of ionic to electronic conductivity (log r) against absolute temperature (T) of the system Li_3PO_4 : *x* Li_3 VO_4

$t \rightarrow \infty$ has been taken as σ_e (electronic contribution) and its value extrapolated to to $\rightarrow 0$ has been taken as total electrical conductivity (σ). The ratio (r) of ionic contribution (σ_i) and electronic contribution (σ_e) to total conductivity (σ) is obtained using the eq. 3.

$$r = \frac{\sigma_i}{\sigma_e} = \frac{\sigma-\sigma_e}{\sigma_e} = \frac{\sigma_{dc}(0)-\sigma_{dc}(\infty)}{\sigma_{dc}(\infty)} \qquad ...(3)$$

The values of r have been evaluated at five to six temperatures from log σ vs t plots for each material. The variation of r with temperature for all the studied material is shown as log r vs T plots in Figs. 7 and 8. It is seen from these plots that in general r increases with temperature which means ionic contribution goes up with T.

In order to check existence of grain boundary or air pares in studied materials, we have measured σ_{dc} (0) and σ_{ac} at frequencies 50 Hz, 100 Hz, 1 kHz, 3kHz and 10kHz at fixed temperature. The results are not shown. It is seen from these figures that there exists no difference between magnitude of dc and ac electrical conductivity. This indicates that grain boundary or air poses are not present in the materials to affect the value of electrical conductivity. This is an expected result as solidified melt has been used for the measurement. Also measured density is found to be very close to X-ray density of the material.

The electronic (σ_e) and ionic (σ_i) part of electrical conductivity have been separated with the help of log r vs T plots. The plots of log $\sigma_i T$ with T^{-1} are shown in Figs. 9 and 10. It is seen from these figures that there is no difference between σ_i and σ at higher temperature (T> 860K) for all the studied material. However, they differ to some extent at lower temperature. These plots are linear and it seems

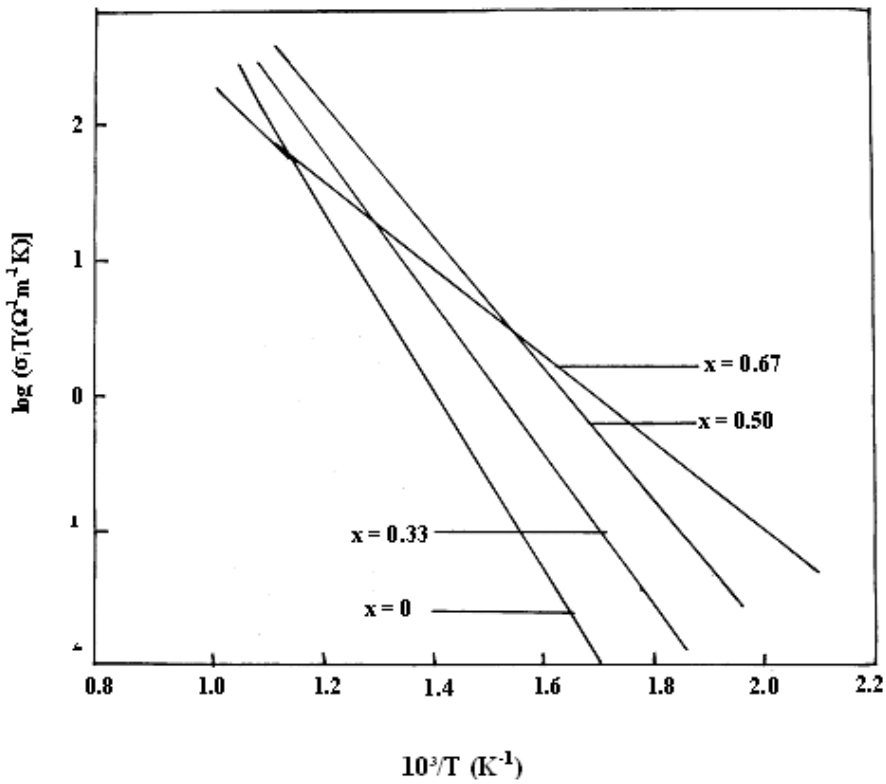

Fig. 9: Plots of logarithm of ionic conductivity (log $\sigma_i T$) against inverse of absolute temperature (T^{-1}) of the system Li_3PO_4 : *x* Li_3 VO_4

that only one type of charge carrier is mobile to give ionic conductivity. The sign of S is positive in this temperature range which indicates that mobile ion is negatively charged or the cations. Li^+ seems to be the mobile species. The value of σ is also high (~ 100 $\Omega^{-1}m^{-1}$) in this temperature range for all the studied material. This is the superionic phase for all the material of the system. The temperature span of superionic phase together with phase transition temperature (T_p) and melting point (T_m) the materials is given in Table 3.

Electrical transport mechanism in superionic phase can be explained on the basis of the values of heat of transport (Q) and activation enthalpy (η_m) for the migration of mobile ion given by eqs. 4 and 5.

$$S = S_{hom} = \frac{Q}{eT} + H \qquad ...(4)$$

...(5)

It is seen from the Tables 1 and 2 that E_a and h are essentially the values of h_m and Q for the mobile ion and also $Q > h_m$ for all the studied solids. Thus the solids may belong to 'rotator' group[18,21]. The lower temperature region is the normal phase of the solids. The variations of electronic conductivity with temperature are not shown. The electronic conductivity also jumps by several order of magnitude at a particular temperature. We have termed it as phase transition temperature (T_p). The sign of S is positive in this region indicating that current carriers are negatively charged. The log $\sigma_e T$ vs T^{-1} plots are linear below this temperature and can be represented by the eq. 6.

...(6)

The values of σ_0, W and linear range of temperature for the studied materials are given in Table 4.

It is seen from the Table that the value of W is large but not enough for the band conduction. Hence electronic conduction may occur due to hopping of electrons trapped at defect centres.

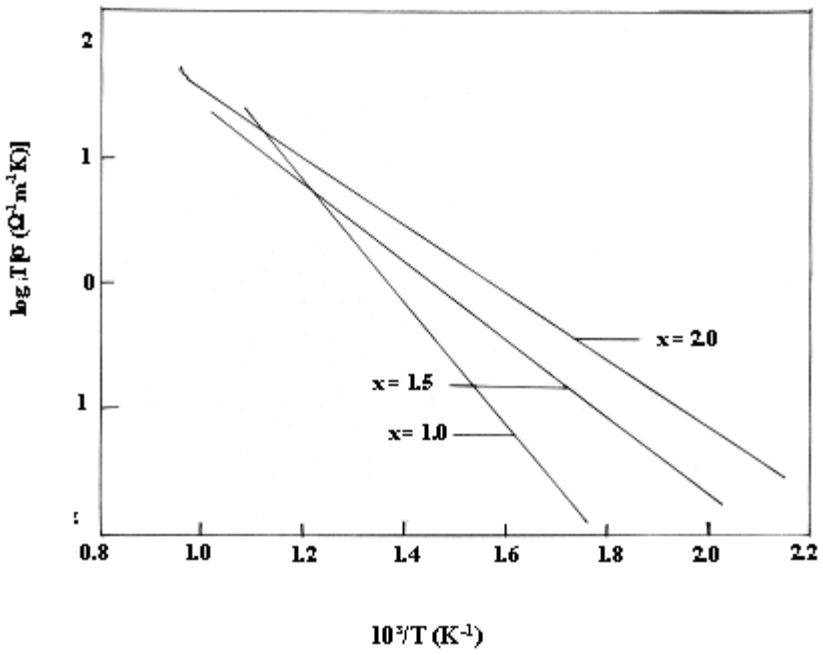

Fig. 10: Plots of logarithm of ionic conductivity (log s_iT) against inverse of absolute temperature (T^{-1}) of the system Li_3PO_4 : *x* Li_3 VO_4

REFERENCES

1. Kvist, A. and Lunden, A., *Natureforsch, Z.,* **20a**: 235 (1965).
2. Idem ibid. **21a**: 1509 (1966).
3. Hu, Y.W., Raistrick, I.D. and Huggins, R.A., *Mater. Res. Bull.* **11**: 1227 (1976).
4. Huggins, R.A., *Electrochim. Acta.,* **22**: 773 (1977).
5. Shanon, R.D., Taylor, B.E., A.D. English and T. Berzins, *Ibid*, **22**: 783 (1977).
6. Jonson, R.T.J. and Biefeld, R.M., in "Fast Ion Transport in solid", edited by Vashishta, P., Mundy, J. and Shenoy, S. (Elsevier North - Holland, Amsterdam, P. 457, (1976).
7. Tuller, H.L., Button, D.P. and Uhlaman, D.R., *J. Non Cryst. Solids.,* **40**: 93 (1980).
8. Shahi, K., Lal, H.B. and Chandra, S., *Indian J. Pure appl. Phys.* **13**: 1 (1973).
9. West, A.R., *J. Appl. Electrochem.,* **3**: 327 (1973).
10. Meghed, S. Madison, WI, (USA), Scorsati, J., B. *Power Sources.,* **79** (1994).
11. Sakurai, Y., Sugihara, S., Shibata, M., Yamaki, *J., Rev* (Japan) **7**: 60 (1995).
12. Ritchie, A.G., Giwa, Co, Lee, JC, Bowles, P., Gil. A. mour, Allan, J., Rice, D.A., Barely, F. Sang, S.C.E. T., *J. Power sources,* **80**: 98 (1999).
13. Wakiharer, M. Mater, *Sci. Eng. R. Rep.* R.**33**: 109 (2001).
14. Takeuchi, E.S. and Haising, R.A., MRS Bull (USA) **27**: 624 (2002).
15. V. Kohler, C. Antonius, P. Bauerlein, *J. Power Sources,* **127**: 45 (2004).
16. Pathak, A.J., Gaur, K. and Lal, H.B., J. *Mater Sci. Lett.* **5**: 785 (1986).
17. Idem,. ibid. **5**: 1058 (1986).
18. Gaur, K., Pathak, A.J. and Lal, H.B., *Ibid*, **7**: 425 (1988).
19. Lal, H.B., Gaur K. and Pathak, A.J., *J. Mater Sci.,* **25**: 3683 (1990).
20. Lal, H.B. and Srivastava, O.P., *J. Mater Sci.,* **77A**: 405 (1983).
21. Aronssin, R., Borjesson, L. and Torvell, L.M., *Phys. Lett.,* **98A**: 205 (1983).